FRAMATOME ANP

BAW-10244
Revision 0

Mark-BW CHF Correlations Applied with XCOBRA-IIIC

September 2003

Framatome ANP, Inc.

Non-Proprietary

BAW-10244
Revision 0

Mark-BW CHF Correlations Applied with XCOBRA-IIIC

by

D. A. Farnsworth and R. L. Harne

Framatome ANP, Inc

Non-Proprietary

U.S. Nuclear Regulatory Commission
Report Disclaimer

Important Notice Regarding the Contents and Use of This Document

Please Read Carefully

This technical report was derived through research and development programs sponsored by Framatome ANP, Inc. It is being submitted by Framatome ANP, Inc. to the U.S. Nuclear Regulatory Commission as part of a technical contribution to facilitate safety analyses by licensees of the U.S. Nuclear Regulatory Commission which utilize Framatome ANP, Inc. fabricated reload fuel or technical services provided by Framatome ANP, Inc. for light water power reactors and it is true and correct to the best of Framatome ANP, Inc.'s knowledge, information, and belief. The information contained herein may be used by the U.S. Nuclear Regulatory Commission in its review of this report and, under the terms of the respective agreements, by licensees or applicants before the U.S. Nuclear Regulatory Commission which are customers of Framatome ANP, Inc. in their demonstration of compliance with the U.S. Nuclear Regulatory Commission's regulations.

Framatome ANP, Inc.'s warranties and representations concerning the subject matter of this document are those set forth in the agreement between Framatome ANP, Inc. and the Customer pursuant to which this document is issued. Accordingly, except as otherwise expressly provided in such agreement, neither Framatome ANP, Inc. nor any person acting on its behalf:

a. makes any warranty, or representation, express or implied, with respect to the accuracy, completeness, or usefulness of the information contained in this document, or that the use of any information, apparatus, method, or process disclosed in this document will not infringe privately owned rights;

   or

b. assumes any liabilities with respect to the use of, or for damages resulting from the use of, any information, apparatus, method, or process disclosed in this document.

Nature of Changes

Item	Page	Description and Justification
Rev. 0		Initial issue.

Contents

Tables

Figures

1.0 Introduction and Summary

This document describes the use of the Framatome ANP BWU CHF correlations (References 1 and 2) in the XCOBRA-IIIC code (Reference 3). The Framatome ANP BWU CHF correlations were previously reviewed and approved in References 1 and 2 for use in Mark-BW fuel assembly design (and the Advanced Mark-BW fuel assembly design which uses the same spacers). The Mark-BW fuel assembly design may contain up to three spacer types and there is a BWU CHF correlation for each spacer type. The BWU-Z correlation is used for the standard spacer with mixing vanes (Reference 1). The BWU-Z correlation with an enhancement factor is used for the region of the assembly which uses the mid-span-mixer (MSM) grids in between the standard mixing vane spacers (Reference 2). The MSM grids may be positioned in between the standard mixing vane spacers in the upper portion of the fuel assembly. The BWU-N correlation (Reference 1) is used for the non-mixing vane spacer, which is in the bottom assembly spacer position.

The LYNXT and XCOBRA-IIIC codes are quite similar. The present versions of both codes for BWU applications utilize the ASME water properties (Reference 5). The primary difference between LYNXT and XCOBRA-IIIC modeling is the treatment of the subchannel hydraulic resistances. LYNXT has the capability for discrete form loss coefficients for each different subchannel type in the bundle being analyzed. XCOBRA utilizes a single average form loss coefficient for all of the subchannels in the bundle. The primary effect is a difference in flow distribution between the subchannels in the bundle. The effects of this difference are discussed in Section 4.1, DNBR 95/95 Limits.

The evaluation of the data base supporting the BWU correlations with XCOBRA-IIIC, rather than with LYNXT, results in a small variation in the DNBR design limits. The DNBR design limit for the BWU-Z correlation in XCOBRA-IIIC is 1.22. The DNBR design limit for the BWU-Z correlation with the enhancement factor for the presence of MSM grids, as implemented in XCOBRA-IIIC, is 1.22. The DNBR design limit for the BWU-N correlation in XCOBRA-IIIC is 1.23. The DNBR design limits approved in References 1 and 2 are a function of pressure. This dependence on pressure has been maintained. The variation of the DNBR design limits with pressure is shown in Section 4.2.

2.0 CHF Test Programs

2.1 *Facility Descriptions*

The tests on the mixing vane spacer addressed in this report were performed at the Columbia University Heat Transfer Research Facility (HTRF). The HTRF is a ten megawatt electric facility capable of testing full length (up to 14 foot heated length) rod arrays in up to a 6 by 6 matrix. HTRF testing conditions cover the full range of operating conditions with pressures up to 2500 psia, mass velocities up to 3.5 million pounds per hour per square foot and inlet temperatures approaching saturation.

The tests on the non-mixing spacer addressed in this report were performed at the Babcock & Wilcox Alliance Research Center (ARC). The ARC facility was similar in capability to the Columbia facility, but has since been decommissioned.

2.2 *Description of Tests*

Individual CHF tests for the Mark-BW Non-MSM spacer, the Mark-BW MSM grid, and the Non-Mixing spacer are summarized in Table 2.1. The test BW 17.0 was not included in the database since it was not included in Reference 1. Complete information, including shroud dimensions, power peaking information, form loss coefficients, etc., are provided in Reference 6 for the Mark-BW spacer tests and Reference 7 for the Non-Mixing spacer tests.

2.3 *Local Conditions Data Analysis*

The bundle and cell geometry, the rod radial peaking values, the heater rod axial flux shape, the axial locations and form losses of spacers, and the thermocouple locations determine the model for each separate test section. The data from each CHF observation within a test consists of the variables test section power, flow, inlet temperature, pressure and CHF location (rod and axial location).

Each test section was modeled for analysis with the XCOBRA-IIIC thermal-hydraulic computer code. A detailed description of this modeling is presented for the Mark-BW spacer in Reference 6 and for the non-mixing spacer in Reference 7.

The XCOBRA-IIIC code produces the local thermal-hydraulic conditions (mass velocity, thermodynamic quality, heat flux, etc.) axially along the test section heated length. The local

condition results at the actual observed location of CHF along with the test section global variables are then compared to the calculated CHF.

Table 2.1 CHF Test Summary

Test	Type {1}	Matrix	Data IDs	AFS {2}	Pin OD Inch	Pitch Inch	G/T OD Inch	Heated Length Inches	Grid Spacing Inches	Hydraulic Diameter Inches
Mark-BW Non-MSM Data (Columbia)										
BW 12.0	Unit	5x5	12xxx	1.55 S	.374	.496	---	143.4	20.5	.4635
BW 13.1	Unit	5x5	131xx	1.55 S	.374	.496	---	143.4	20.5	.4635
BW 14.1	G-T	5x5	141xx	1.55 S	.374	.496	.482	143.4	20.5	.3747
BW 15.1	C-U	5x5	151xx	1.55 S	.374	.496	.374	143.4	20.5	.4635
BW 16.0	C-R	5x5	16xxx	1.55 S	.374	.496	.374	143.4	20.5	.4635
BW 17.0	W-H	5x5	17xxx	1.55 S	.374	.496	---	143.4	20.5	.4635
BW 19.0	G-T	5x5	19xxx	1.55 S	.374	.496	.482	143.4	20.5	.3747
BW 20.0	SLB	5x5	20xxx	1.55 S	.374	.496	---	143.4	20.5	.4635
Mark-BW MSM Data (Columbia)										
BW 18.0	MSM	5x5	18xxx	1.55 S	.374	.496	---	143.4	{3}20.5	.4635
BW 18.1	MSM	5x5	181xx	1.55 S	.374	.496	---	143.4	{3}20.5	.4635
BW 43.0	G-T	5x5	43xxx	1.55 S	.374	.496	.482	143.4	{3}20.5	.3747
BWU-N Non-Mixing Grid Data (ARC)										
C – 3	Unit	3x3	73xxx	Uniform	.379	.501	---	72.0	20.5	.4642
C – 6	Unit	5x5	76xxx	Uniform	.379	.501	---	144.0	20.5	.4642
C – 7	G-T	5x5	77xxx	Uniform	.379	.501	.465	144.0	20.5	.3940
C – 8	Unit	5x5	78xxx	1.66 S	.379	.501	---	144.0	20.5	.4642
C – 9	G-T	5x5	79xxx	1.66 S	.379	.501	.465	144.0	20.5	.3940
C – 11	Unit	5x5	81xxx	1.60 Out	.379	.501	---	144.0	20.5	.4642
C – 12	G-T	5x5	82xxx	1.60 Out	.379	.501	.465	144.0	20.5	.3940
B – 16	Unit	5x5	86xxx	1.66 S	.430	.568	---	144.0	20.5	.5353
B – 17	G-T	5x5	87xxx	1.66 S	.430	.568	.554	144.0	20.5	.4238
B – 18	Int	5x5	88xxx	1.66 S	.430	.590	---	144.0	20.5	.6007

{1} – G-T = Guide Tube, C-U = Cold Unit, C-R = Cold Row, Int = Intersection, MSM = mid-span-mixer, SLB = Steam Line Break Conditions (Unit), W-H = Water Hole (rod moved)
{2} – S = Symmetric, Out = Outlet
{3} – Non-structural mixing grid at last 3 midspans

Note that BW 17.0 is not included in the database.

3.0 The BWU-Z and BWU-N CHF Correlations

The development and justification for the BWU correlations are described in References 1 and 2. The form of the correlation has been implemented into XCOBRA-IIIC unchanged from that in References 1 and 2.

The form for the uniform part of the BWU CHF correlation is defined as

$$
\begin{aligned}
Q_{unif} = {} & A_0 \bullet X_0 + A_1 \bullet X_1 + A_2 \bullet X_2 + A_3 \bullet X_3 \\
& + A_4 \bullet X_4 + A_5 \bullet X_5 + A_6 \bullet X_6 \\
& + A_7 \bullet X_7 + A_8 \bullet X_8 + A_9 \bullet X_9 \\
& + A_{10} \bullet X_{10} + A_{11} \bullet X_{11} + A_{12} \bullet X_{12} + A_{13} \bullet X_{13}
\end{aligned}
$$

or $$Q_{unif} = SUM[A_i \bullet X_i]i = 0,13$$

where

The FLS and F factors are defined as:

$$FLS = C_1 + C_2 \bullet L + C_3 \bullet S + C_4 \bullet L \bullet S + C_5 \bullet L^2 + C_6 \bullet S^2$$

and

$$F = \frac{K \bullet q''_{av}}{q''_{l}\left(1-e\right)^{K \bullet l_c}} \int_0^{l_c} \left[f\left(z\right)\right] e^{-K\left(l_c - z\right)} dz$$

$$K = \frac{B_1\left(1-X\right)^{B_2}}{\left(G/10^6\right)^{B_3}}$$

where

L = heated (active) length, inches

S = spacer grid spacing (pitch), inches

l_c = axial location of CHF, inches

q''_{av} = rod average flux, Btu/hr-ft^2

$f\left(z\right)$ = local to average heat flux ratio

q''_{l} = local heat flux, Btu/hr-ft^2

Finally, a performance factor, PF, is applicable to all designs. The base performance factor is 1.0. Spacer designs using the same basic equation but exhibiting a uniform increase or decrease in CHF over the range of independent variables may have a performance factor differing from 1.0.

Thus,

$$Q_{chf} = PF*FLS*Q_{unif}/F$$

The FLS factor was developed in Reference 1 to accurately correlate the spacer spacing and heated length effects associated with a mixing vane spacer. There is no corresponding spacer or heated length effects for Non-Mixing spacers. Therefore, the FLS factor is set to unity for the Non-Mixing spacer.

3.1 *The BWU Coefficients*

The individual BWU coefficients for the Mark-BW Non-MSM spacer, the Mark-BW MSM grid , and the Non-Mixing spacer are shown in Table 3.1. These coefficients were optimized for their respective databases in References 1 and 2 using the methods described in References 8, 9, and 10. The form of the correlation and the values of the coefficients were approved in References 1 and 2 for use with the LYNXT code.

3.2 *Results and Verification*

The individual local condition results from analyses of the data with XCOBRA-IIIC are tabulated in Appendices A, B, and C for the respective databases. The overall statistics for each database are presented in Tables 3.2 through 3.4. The statistical parameters presented in Tables 3.2 through 3.4 are the same as those utilized in Reference 1.

It is important to check the individual results for bias with respect to either the dependent or any of the independent variables in the development and verification of any correlation. A visual representation is convenient for the local conditions (heat fluxes, mass velocities, pressures and qualities). Tabular comparisons are necessary for the bundle global variables such as cell type, grid spacing, etc., as well as mass velocity, pressure and quality.

An examination of the plots of the measured to predicted (M/P) CHF ratio against the independent variables of mass velocity, pressure and quality for each grid type shows that there is no major deviation from a horizontal line and thus no independent variable bias. These results are shown in Figures 3.1 through 3.3 for the Mark-BW Non-MSM spacer, Figures 3.6 through 3.8 for the Mark-BW MSM grid and Figures 3.11 through 3.13 for the Non-Mixing spacer database.

Scatter plots of the measured CHF against the predicted CHF with the BWU correlation (the dependent variable) are presented for each of the designs in turn (Mark-BW Non-MSM, Mark-BW MSM and Non-Mixing Grid) (Figures 3.4, 3.9, and 3.14). There are no significant deviations of the data grouping about the 45 degree line for any of the cases and thus there is no dependent variable bias.

Figures 3.5, 3.10, and 3.15 present histograms of the individual M/P results, confirming the normal (or quasi normal for the Non-Mixing spacer, Figure 3.15) distribution of the database for each design type.

Tabular comparisons on a M/P basis against all appropriate independent variables for each of the fuel designs in turn are presented in Tables 3.5 through 3.7. Close examination of these tables shows the good coherence over each of the applicable variable ranges for each of the different designs. None of the groupings (with at least 20 data points) are outside the traditionally accepted 5% CHF uncertainty band.

Table 3.1 BWU Coefficients (Reference 1)

Table 3.2 Descriptive Statistics and D Prime Test
Mark-BW Non-MSM Database BWU-Z Correlation

DATA FILE	XCANON.DAT	# OF DATA	530
MAX VALUE	0.128970D+01	MIN VALUE	0.706100D+00
RANGE	0.583600D+00	MEDIAN	0.983900D+00
MEAN	0.981341D+00	STD DEV	0.886121D -01
SKEWEDNESS	-.150824D+00	KURTOSIS	-.124282D+00
UPPER D'	0.346900D+04	LOWER D'	0.340700D+04
DPRIME VAL	0.345119D+04	ACCEPT NORMALITY AT 5% LEVEL	

Descriptive Statistics - Reference 11
D Prime - Reference 12

Table 3.3 Descriptive Statistics and D Prime Test
Mark-BW MSM Database BWU-Z Correlation

DATA FILE	XCAMSM.DAT	# OF DATA	148
MAX VALUE	0.118190D+01	MIN VALUE	0.735000D+00
RANGE	0.446900D+00	MEDIAN	0.974400D+00
MEAN	0.980401D+00	STD DEV	0.847316D -01
SKEWEDNESS	0.311436D -01	KURTOSIS	-.285871D+00
UPPER D'	0.515040D+03	LOWER D'	0.497820D+03
DPRIME VAL	0.509699D+03	ACCEPT NORMALITY AT 5% LEVEL	

Descriptive Statistics - Reference 11
D Prime - Reference 12

Table 3.4 Descriptive Statistics and D Prime Test
Non-Mixing Database BWU-N Correlation

DATA FILE	all-bwun.dat	# OF DATA	1093
MAX VALUE	0.146710D+01	MIN VALUE	0.659300D+00
RANGE	0.807800D+00	MEDIAN	0.996300D+00
MEAN	0.993156D+00	STD DEV	0.103106D+00
SKEWEDNESS	-.651307D -01	KURTOSIS	0.537658D+00
UPPER D'	0.102524D+05	LOWER D'	0.101234D+05
DPRIME VAL	0.100869D+05	REJECT NORMALITY AT 5% LEVEL	

Descriptive Statistics - Reference 11
D Prime - Reference 12

Table 3.5 M/P CHF Performance by Independent Variable Grouping Mark-BW Non-MSM Database with BWU-Z

**Table 3.6 M/P CHF Performance by Independent Variable Grouping
Mark-BW MSM Database with BWU-Z**

Table 3.7 M/P CHF Performance by Independent Variable Grouping Non-Mixing Database with BWU-N

Figure 3.1

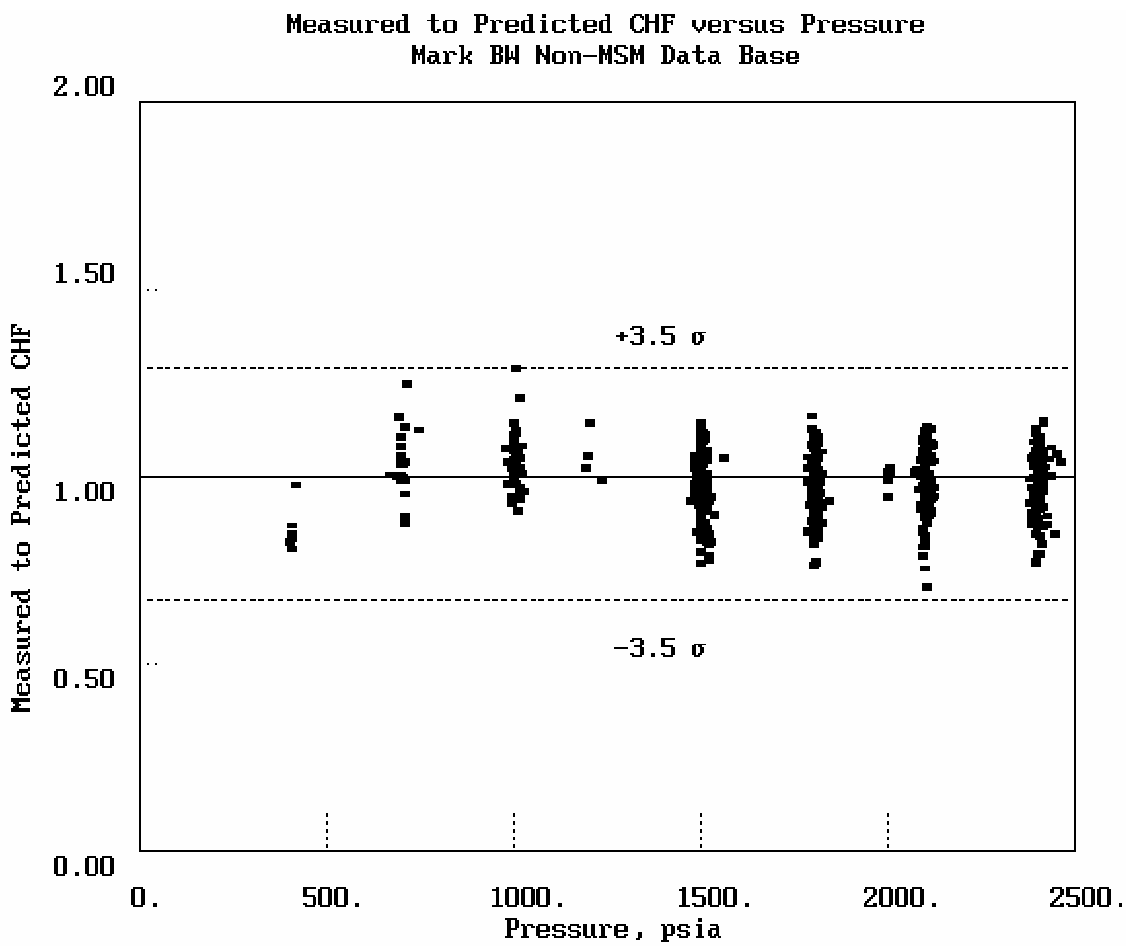
Measured to Predicted CHF versus Pressure
Mark BW Non-MSM Data Base
Measured to Predicted CHF
Pressure, psia
+3.5 σ
-3.5 σ
2.00
1.50
1.00
0.50
0.00
0.
500.
1000.
1500.
2000.
2500.

Figure 3.2

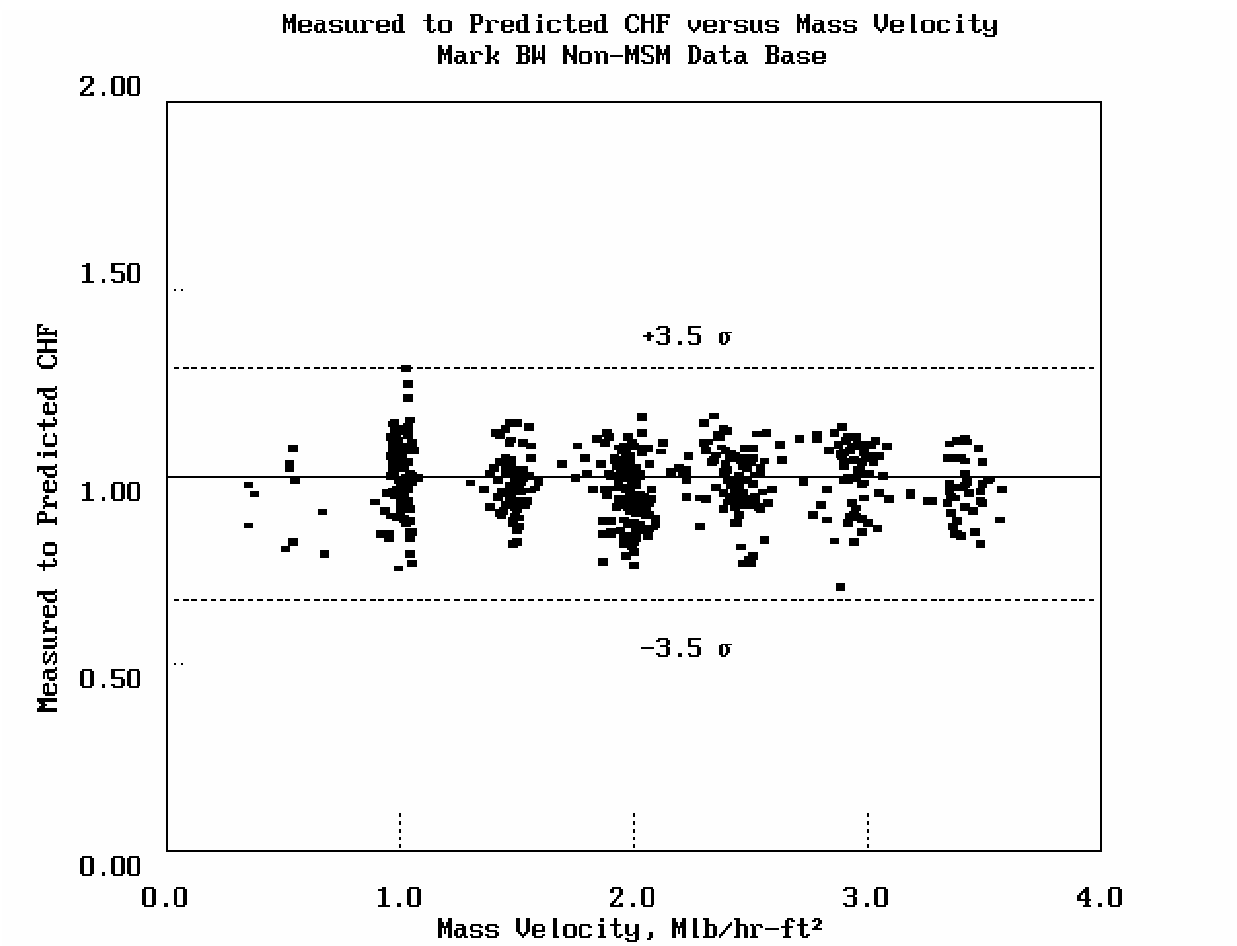
Measured to Predicted CHF versus Mass Velocity
Mark BW Non-MSM Data Base
2.00
1.50
1.00
0.50
0.00
Measured to Predicted CHF
+3.5 σ
-3.5 σ
0.0
1.0
2.0
3.0
4.0
Mass Velocity, Mlb/hr-ft²

Figure 3.3

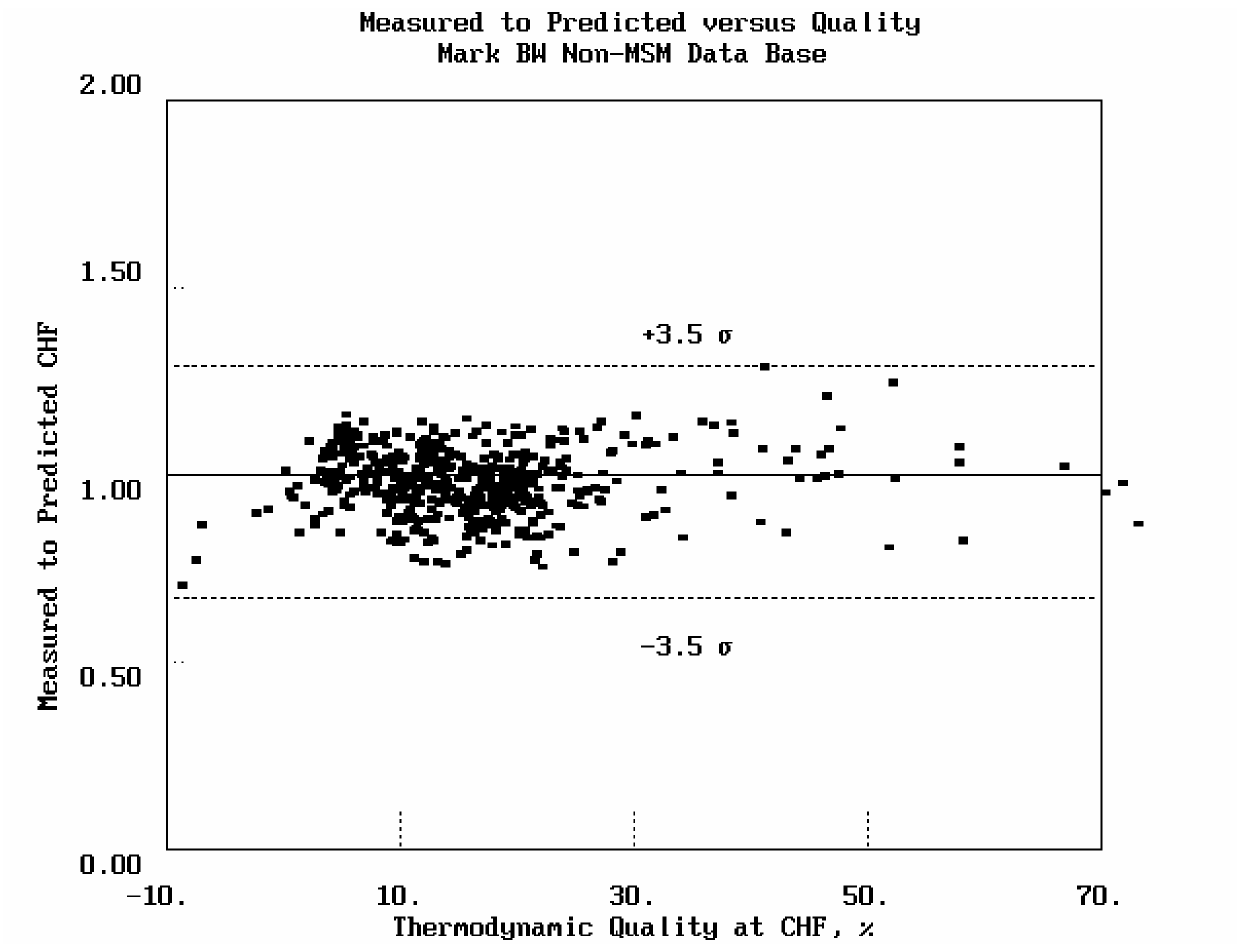
Measured to Predicted versus Quality
Mark BW Non-MSM Data Base
2.00
1.50
1.00
0.50
0.00
+3.5 σ
-3.5 σ
Measured to Predicted CHF
-10.
10.
30.
50.
70.
Thermodynamic Quality at CHF, %

Figure 3.4

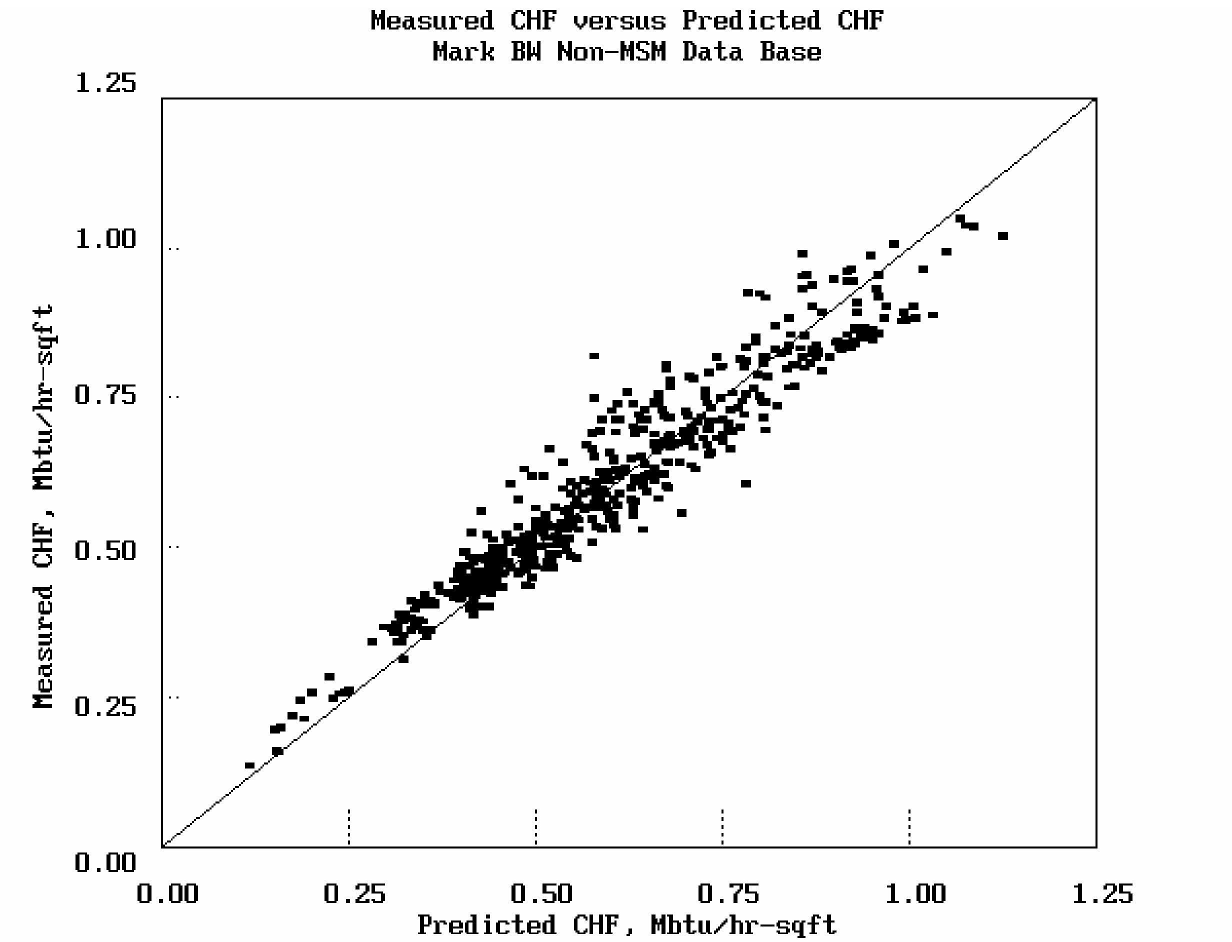
Measured CHF versus Predicted CHF
Mark BW Non-MSM Data Base
1.25
1.00
0.75
0.50
0.25
0.00
Measured CHF, Mbtu/hr-sqft
0.00
0.25
0.50
0.75
1.00
1.25
Predicted CHF, Mbtu/hr-sqft

Figure 3.5

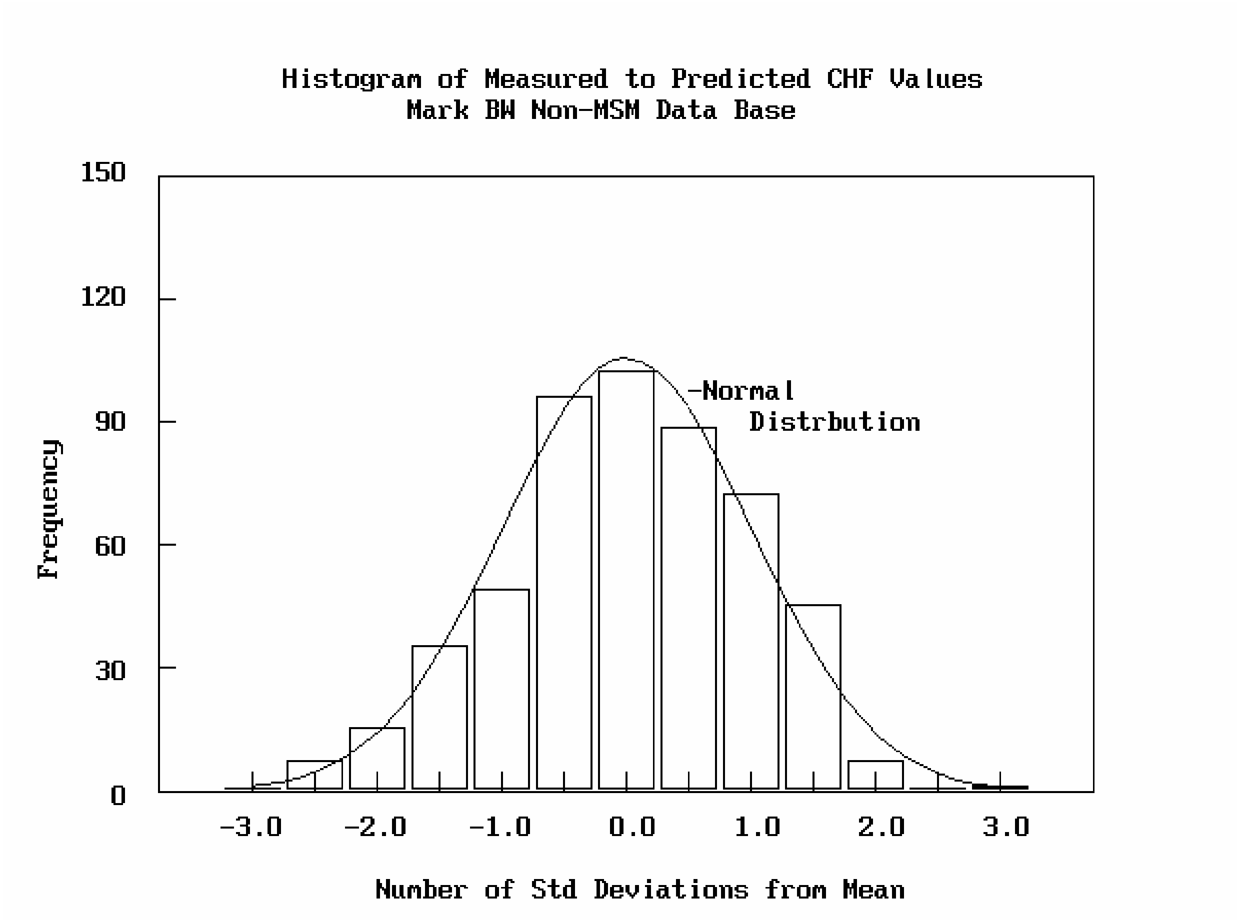
Histogram of Measured to Predicted CHF Values
Mark BW Non-MSM Data Base
150
120
90
60
30
0
Frequency
-Normal
Distrbution
-3.0
-2.0
-1.0
0.0
1.0
2.0
3.0
Number of Std Deviations from Mean

Figure 3.6

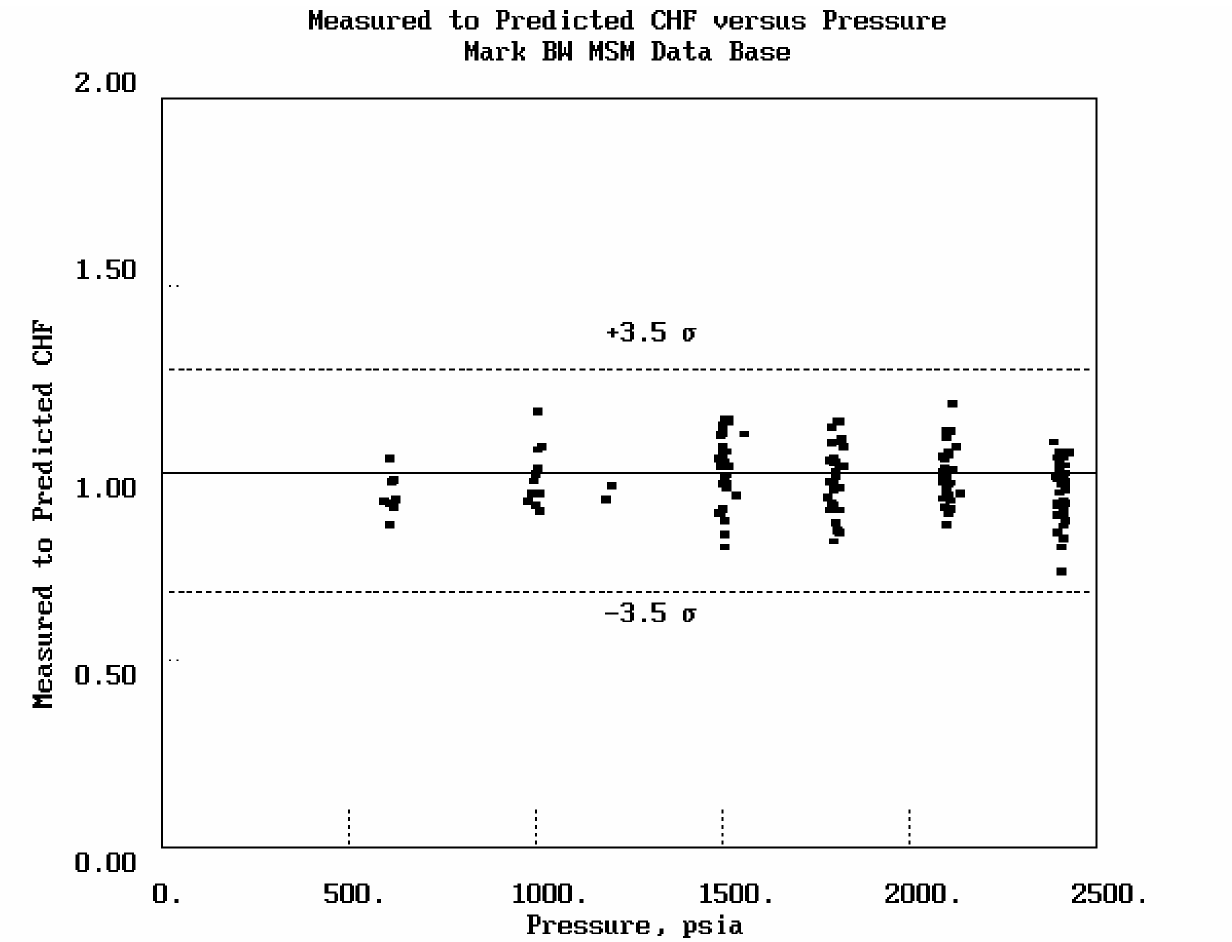
Measured to Predicted CHF versus Pressure
Mark BW MSM Data Base
2.00
1.50
1.00
0.50
0.00
Measured to Predicted CHF
+3.5 σ
−3.5 σ
0.
500.
1000.
1500.
2000.
2500.
Pressure, psia

Figure 3.7

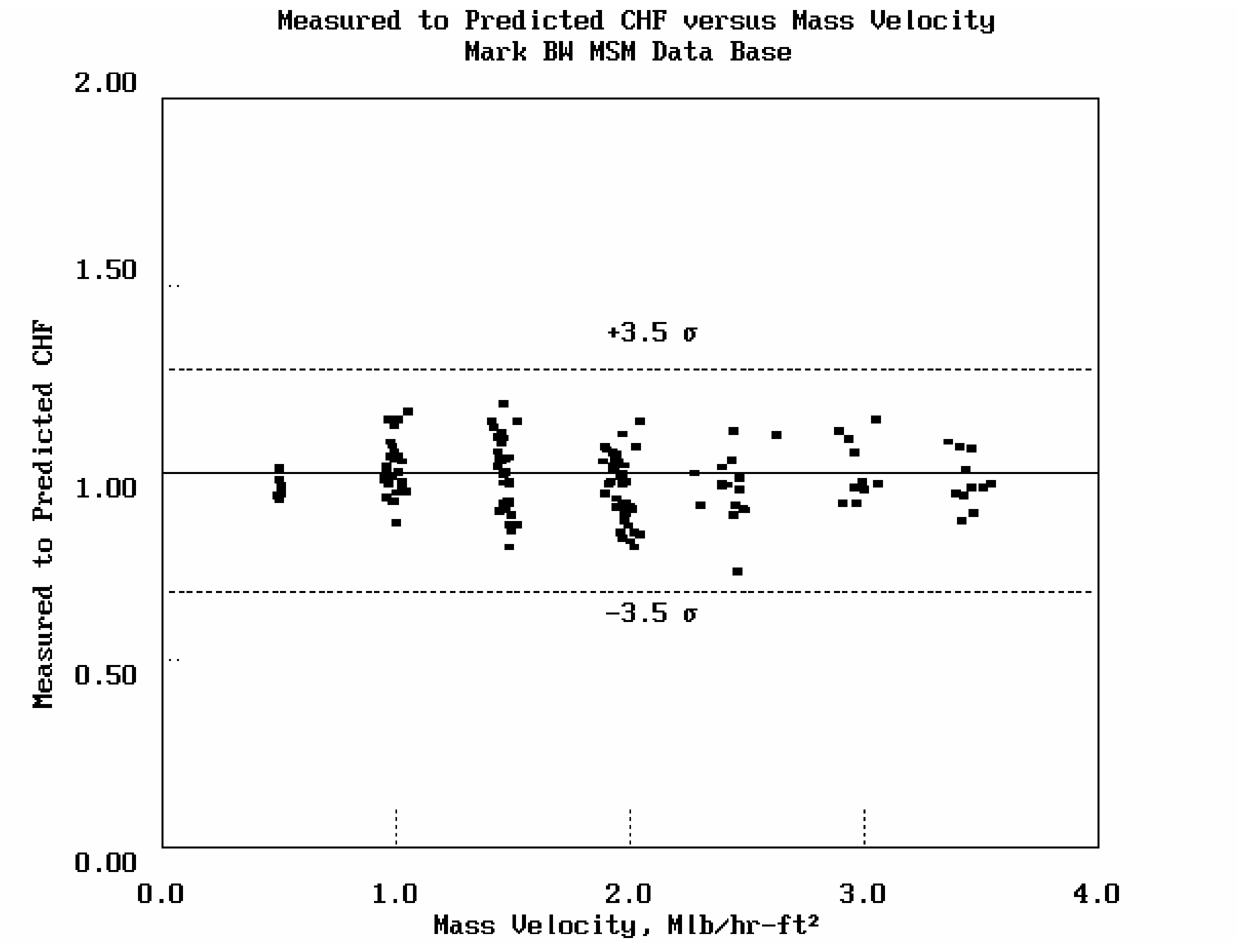
Measured to Predicted CHF versus Mass Velocity
Mark BW MSM Data Base
2.00
1.50
1.00
0.50
0.00
+3.5 σ
-3.5 σ
Measured to Predicted CHF
0.0
1.0
2.0
3.0
4.0
Mass Velocity, Mlb/hr-ft²

Figure 3.8

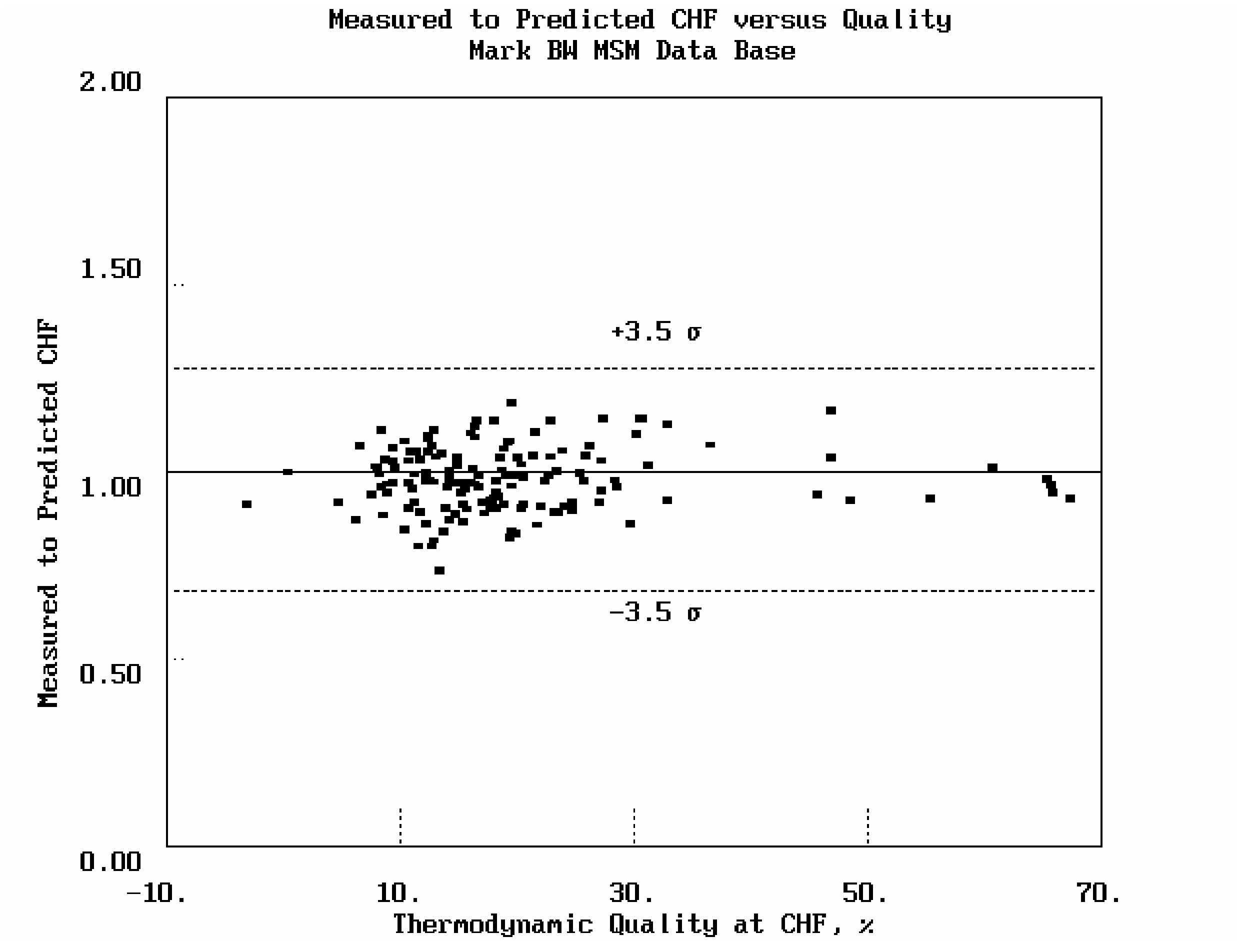
Measured to Predicted CHF versus Quality
Mark BW MSM Data Base
Measured to Predicted CHF
2.00
1.50
1.00
0.50
0.00
+3.5 σ
−3.5 σ
−10.
10.
30.
50.
70.
Thermodynamic Quality at CHF, %

Figure 3.9

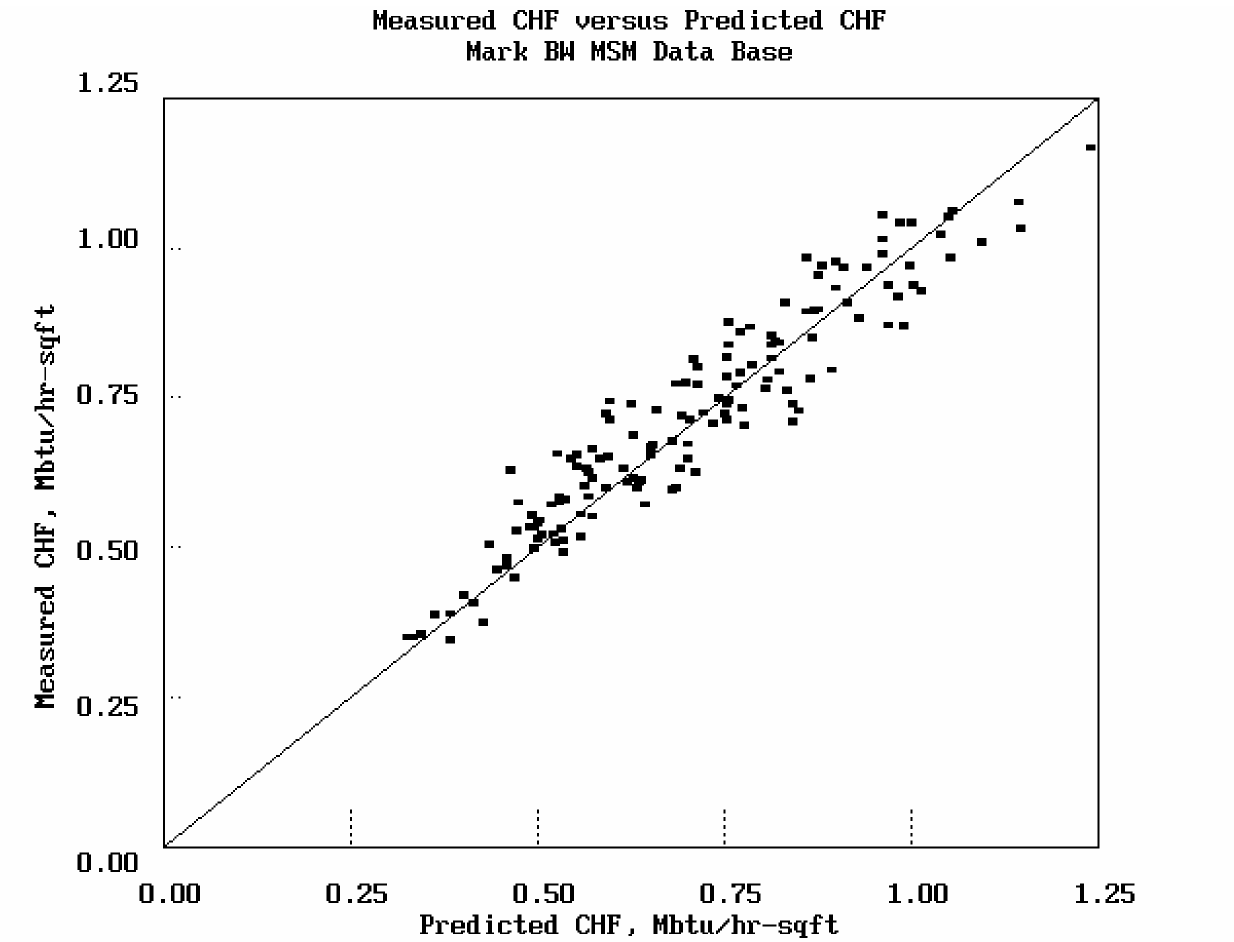
Measured CHF versus Predicted CHF
Mark BW MSM Data Base
1.25
1.00
0.75
0.50
0.25
0.00
Measured CHF, Mbtu/hr-sqft
0.00
0.25
0.50
0.75
1.00
1.25
Predicted CHF, Mbtu/hr-sqft

Figure 3.10

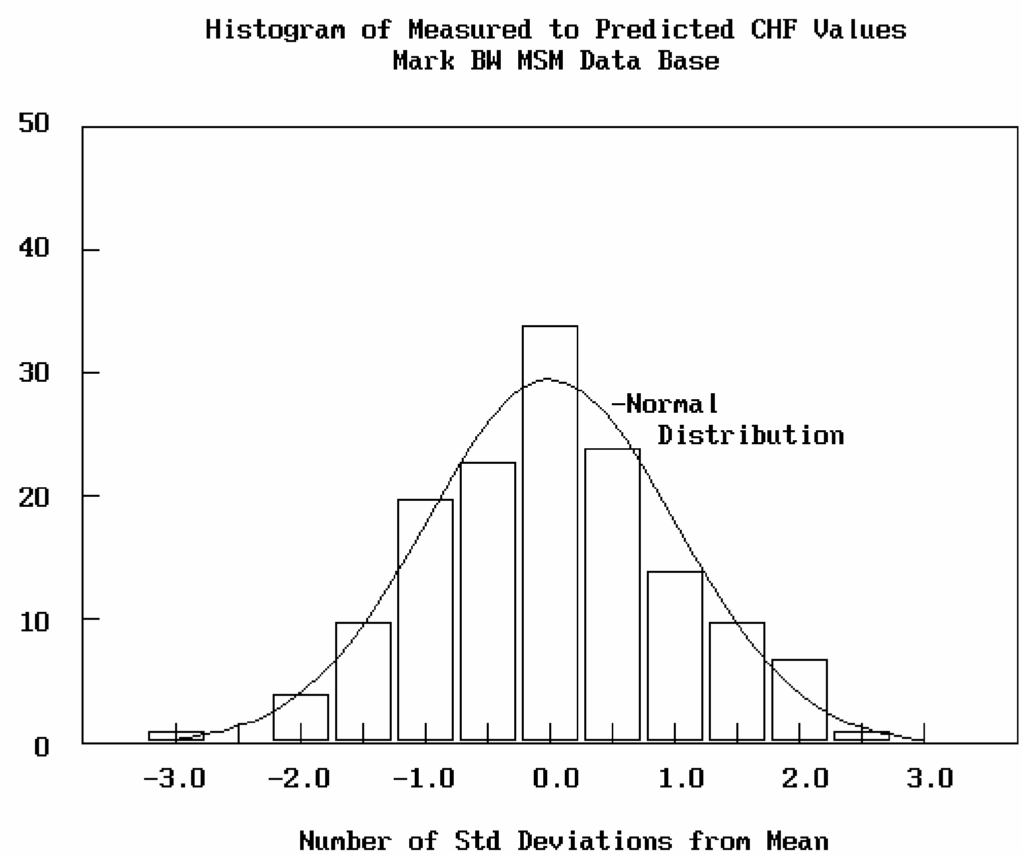
Histogram of Measured to Predicted CHF Values
Mark BW MSM Data Base
50
40
30
20
10
0
-Normal
Distribution
-3.0
-2.0
-1.0
0.0
1.0
2.0
3.0
Number of Std Deviations from Mean

Figure 3.11

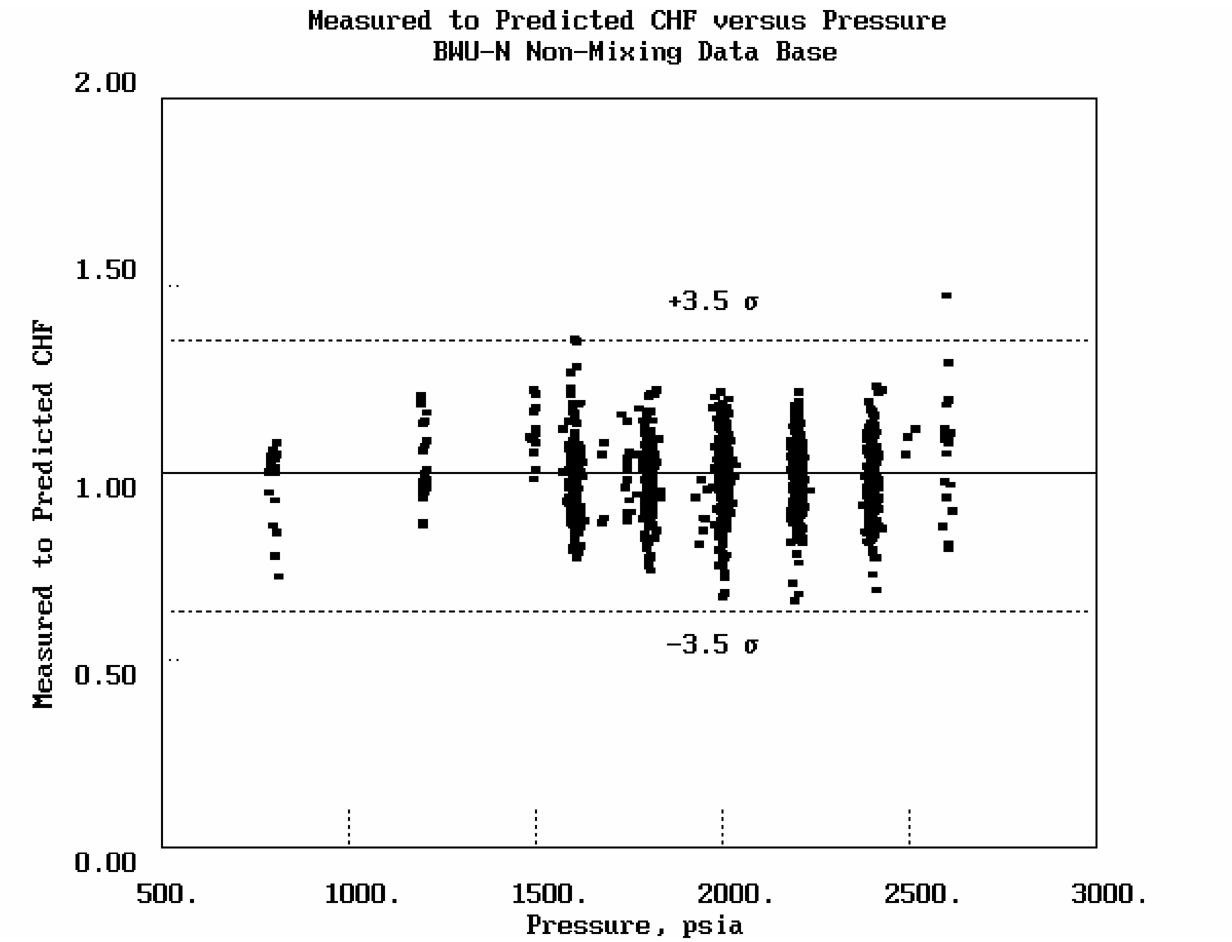
Measured to Predicted CHF versus Pressure
BWU-N Non-Mixing Data Base
Measured to Predicted CHF
Pressure, psia
2.00
1.50
1.00
0.50
0.00
500.
1000.
1500.
2000.
2500.
3000.
+3.5 σ
-3.5 σ

Figure 3.12

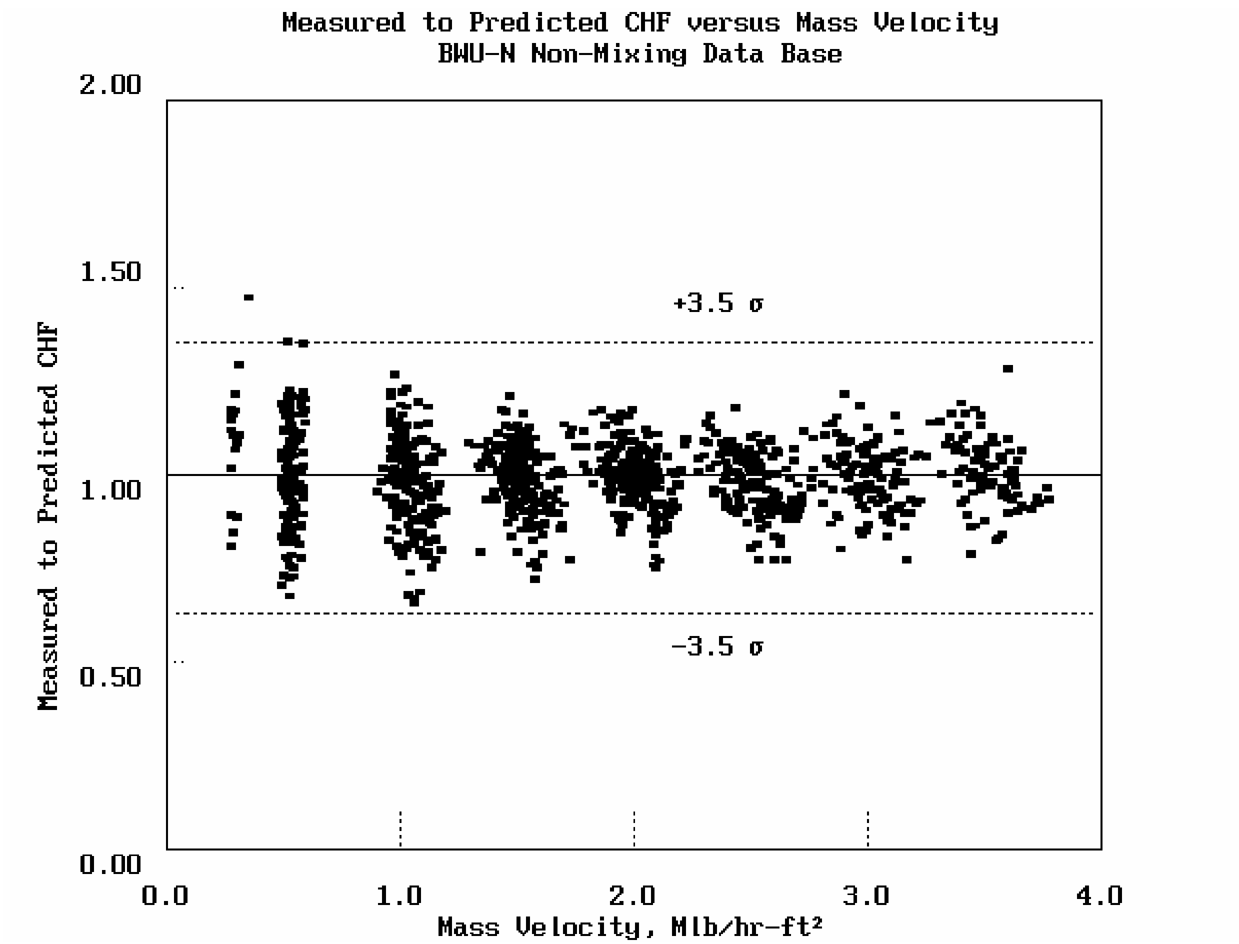
Measured to Predicted CHF versus Mass Velocity
BWU-N Non-Mixing Data Base
2.00
1.50
1.00
0.50
0.00
Measured to Predicted CHF
+3.5 σ
-3.5 σ
0.0
1.0
2.0
3.0
4.0
Mass Velocity, Mlb/hr-ft²

Figure 3.13

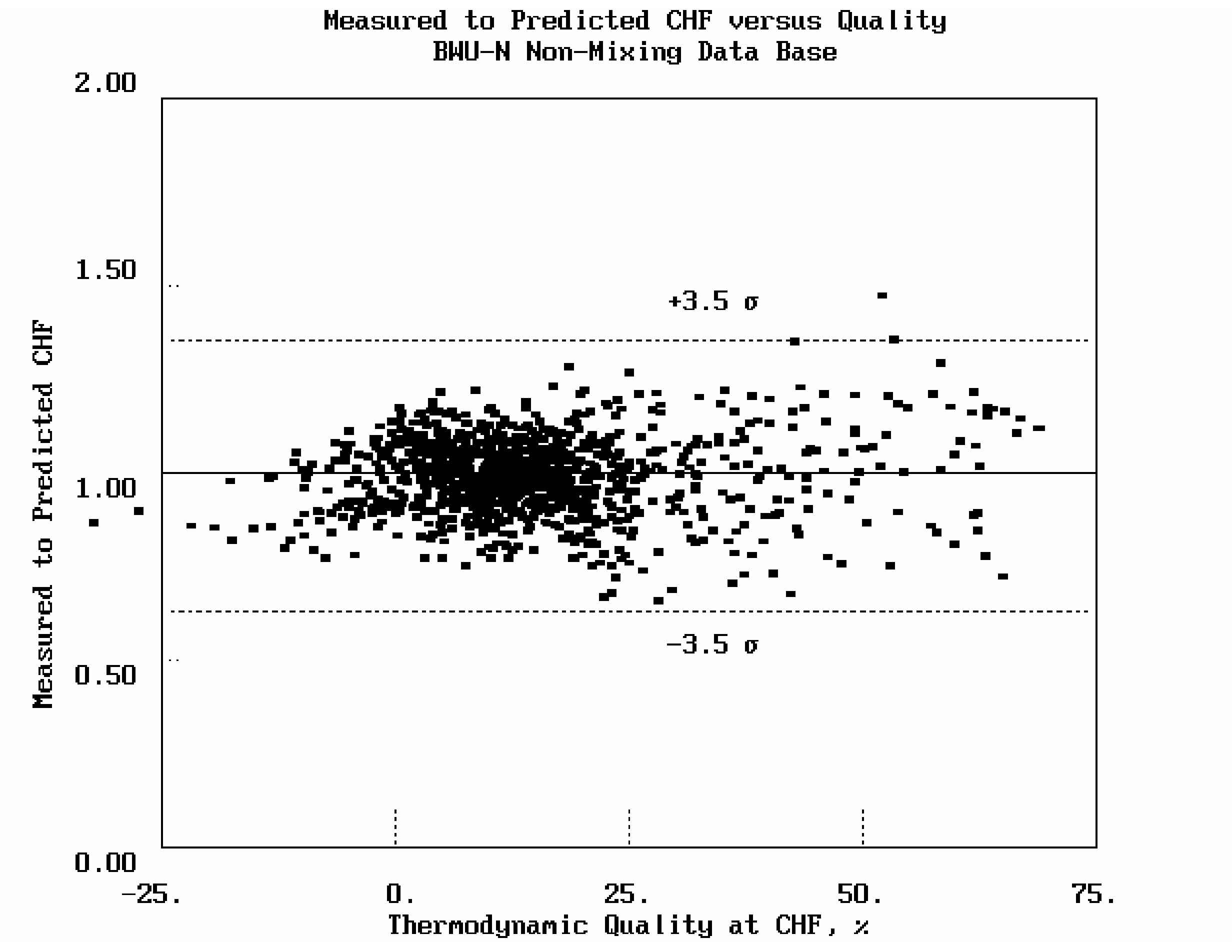
Measured to Predicted CHF versus Quality
BWU-N Non-Mixing Data Base
2.00
1.50
1.00
0.50
0.00
Measured to Predicted CHF
+3.5 σ
-3.5 σ
-25.
0.
25.
50.
75.
Thermodynamic Quality at CHF, %

Figure 3.14

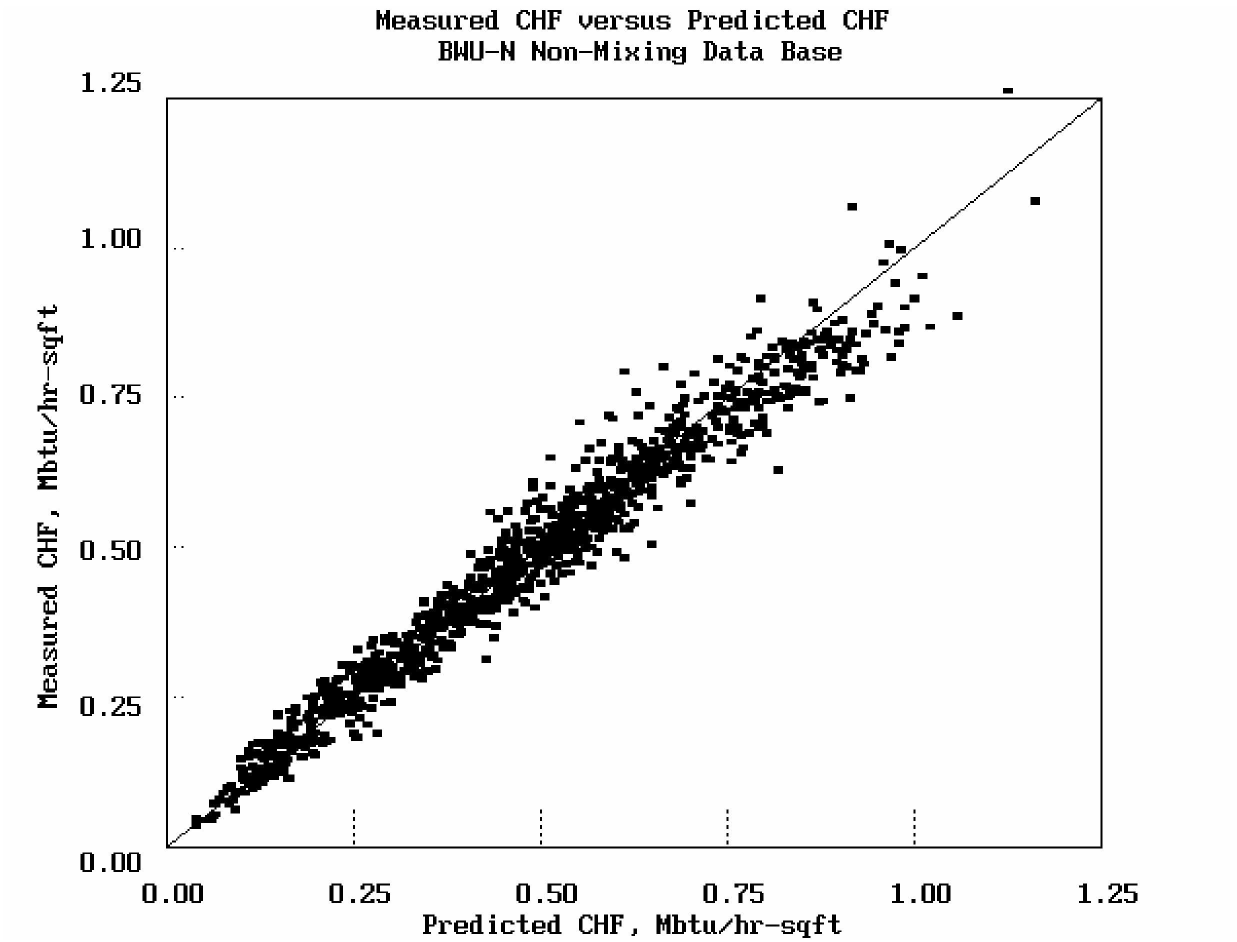
Measured CHF versus Predicted CHF
BWU-N Non-Mixing Data Base
Measured CHF, Mbtu/hr-sqft
Predicted CHF, Mbtu/hr-sqft
0.00
0.25
0.50
0.75
1.00
1.25

Figure 3.15

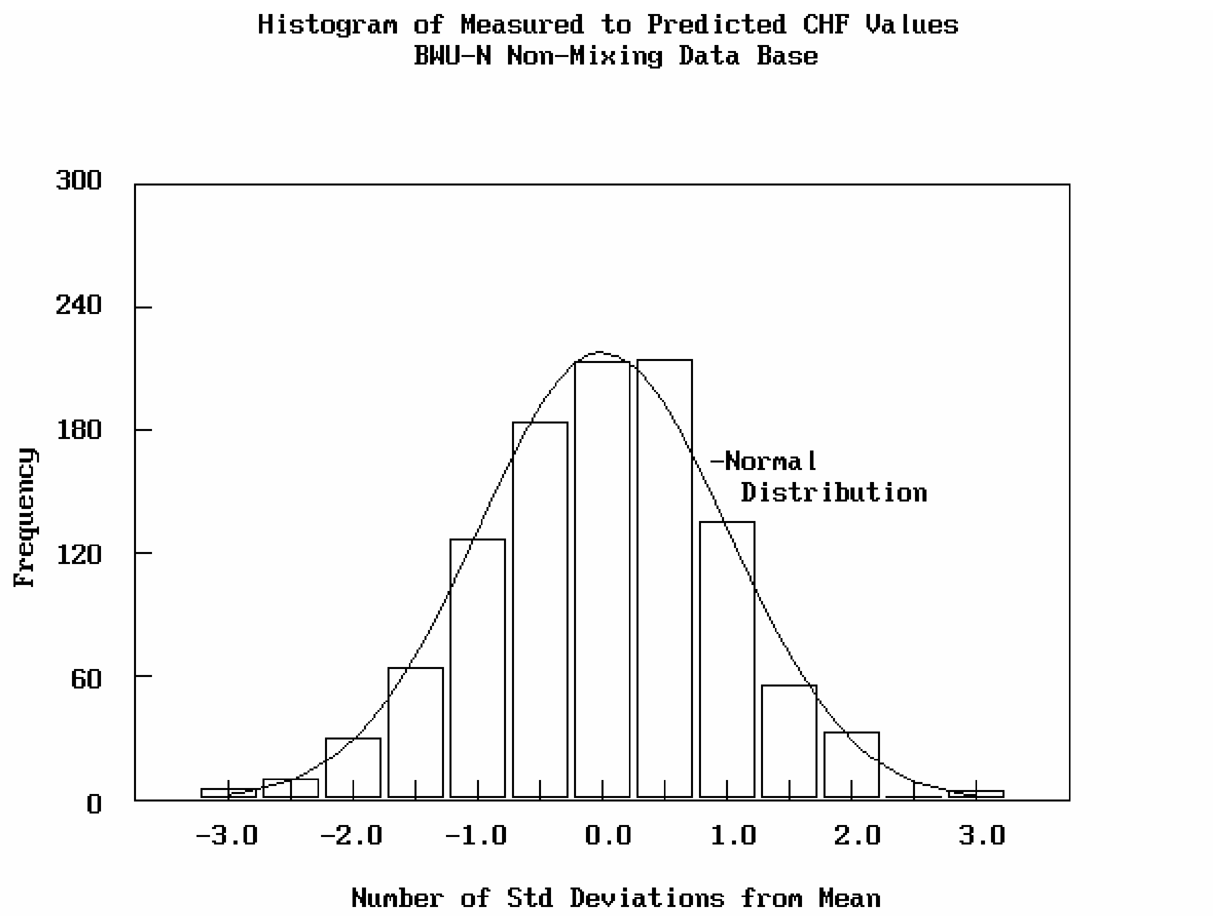
Histogram of Measured to Predicted CHF Values
BWU-N Non-Mixing Data Base
300
240
180
120
60
0
Frequency
-Normal
Distribution
-3.0
-2.0
-1.0
0.0
1.0
2.0
3.0
Number of Std Deviations from Mean

4.0 DNBR Design Limits

The use of CHF equations in pressurized water reactor analyses is facilitated by the definition of the Departure from Nucleate Boiling Ratio (DNBR):

$$\mathrm{DNBR} = \frac{q''_{CHF}}{q''_{Actual}} = \frac{\text{calculated CHF at a given location}}{\text{actual heat flux at that location}}$$

The DNBR is a measure of the local thermal margin to film boiling. A DNBR value of 1.0 implies transition to film boiling at that location. The higher the DNBR (above 1.0), the greater the margin to film boiling.

In design analyses, DNBR values are calculated throughout the core for a given core condition. Calculation of the minimum core DNBR and comparison of this minimum with a design limit ($DNBR_L$) provides protection against departure from nucleate boiling in the core. The $DNBR_L$ is the lowest DNBR that can be calculated (for any given core condition) on the limiting fuel rods in the reactor while still maintaining a 95 percent confidence that 95 percent of these limiting fuel rods are not in film boiling.

The CHF is calculated using a correlation (BWU in this case), and thus an uncertainty in this calculation exists based on the precision of the correlation. Using the one-sided tolerance theory from Owen (Reference 13), a lower tolerance value of predicted CHF can be defined for a given confidence and population coverage:

$$q''_{CL} = q''_{c}\left(M/P - K_{N,C,P} \bullet s_{M/P}\right)$$

where

q''_{CL} = lower tolerance limit of calculated CHF

q''_{c} = calculated CHF from the correlation

M/P = mean measured CHF to predicted CHF ratio for the correlation database

$s_{M/P}$ = the standard deviation of the measured to predicted ratios of the database

$K_{N,C,P}$ = one-sided tolerance factor based on degrees of freedom (N), confidence level (C), and portion of population covered (P)

Equating the maximum allowable design heat flux (q''_{ND}) to the lower limit CHF (q''_{CL}), the design limit DNBR can be determined:

$$q''_{ND} = q''_c \bullet \left(M/P - K_{N,C,P} \bullet \sigma_{M/P}\right)$$

$$DNBR_L = \frac{q'_c}{q'_{ND}} = \frac{1}{M/P - K_{N,C,P} \bullet s_{M/P}}$$

Thus, DNBR values greater than the $DNBR_L$ provide assurance (with appropriate confidence and population coverage) that no film boiling exists.

4.1 ***DNBR 95/95 Limits***

The BWU design limit for each of the BWU correlations is developed following the approach described above. N is the appropriate value for the number of degrees of freedom for a design limit. The standard deviation, σ, is based on n-1. Thus the correction is:

$$s_N \left(\text{corrected for N}\right) = s_{M/P} \bullet \left[(n-1)/N\right]^{1/2}.$$

For the Mark-BW database, using the BWU-Z correlation and the data from Table 3.2,

n, # of data	530
N, degrees of freedom (n-1-14)	515
M/P, avg measured to predicted CHF	0.9813
$s_{M/P}$	0.0866
s_N (corrected for N)	0.0898
K (500, 0.95, 0.95), one sided tolerance factor (Reference 11)	1.762

The number of degrees of freedom, N, has been reduced by the number of coefficients in the correlation used to fit the data (14).

The Mark-BW BWU-Z design limit is:

$$DNBR(L) = 1/\left(M/P - K \bullet s_N\right)$$

$$= 1/\{0.9813 - 1.762(0.0898)\} = 1.215 \rightarrow 1.22$$

For the Mark-BW MSM database, using the BWU-Z correlation with a performance factor of [ ] and the data from Table 3.5,

n, # of data	148
N, degrees of freedom (n-1)	147
M/P, avg measured to predicted CHF	0.9804
$s_{M/P}$	0.0847
s_N (corrected for N)	0.0847
K (148, .95, 0.95), one sided tolerance factor (Reference 11)	1.872

The Mark-BW MSM data was not used to develop the BWU-Z CHF correlation and thus no correction for the number of coefficients is needed.

The Mark-BW MSM design limit is:

$$DNBR(L) = 1/(M/P - K \bullet s_N)$$

$$= 1 / \{0.9804 - 1.872\ (.0847)\} = 1.217 \rightarrow 1.22$$

For the Non-Mixing database, using the BWU-N correlation and the data from Table 3.6,

n, # of data	1093
N, degrees of freedom (n-1-14)	1078
M/P, avg measured to predicted CHF	0.9932
$s_{M/P}$	0.1031
s_N (corrected for N)	0.1038
K (1093, 0.95, 0.95), one sided tolerance factor (Reference 11)	1.724

The Non-Mixing BWU-N design limit is:

$$DNBR(L) = 1/(M/P - K \bullet s_N)$$

$$= 1 / \{0.9932 - 1.724(.1038)\} = 1.228 \rightarrow 1.23$$

The distribution of the M/P values for the BWU-N correlation is treated as normal for the purpose of defining the 95/95 limit even though the distribution fails the normality test as shown in Table 3.4. The distribution is close to normal as the table and Figure 3.15 indicate. Based on these observations, the treatment of the BWU-N data base as a normal distribution was accepted in Reference 1 where it was also found to be slightly non-normal.

The design limits for each of the BWU correlations as used in XCOBRA-IIIC are larger than those developed in Reference 1 using the LYNXT code. This is almost entirely due to the different form loss coefficient modeling between LYNXT and XCOBRA-IIIC. LYNXT models each subchannel in the 5x5 bundle with discrete form loss coefficients. XCOBRA-IIIC uses the same form loss coefficient, representing the spacer form loss coefficient, across all the subchannels in the 5x5 test bundle. The impact of using non-discrete form losses in the correlation verification using XCOBRA-IIIC results in a slightly higher CHF design limit as compared to LYNXT based results. The impact of using non-discrete form loss coefficients in the subsequent CHF correlation application results in slightly less severe DNBR predictions. The combined impacts of using non-discrete form loss coefficients with XCOBRA-IIIC during correlation verification and application are essentially offsetting.

4.2 *Correlation Applicability and DNBR Limits vs. Pressure*

The ranges of applicability for the BWU correlations are shown in Tables 4.1 through 4.3 for the Mark-BW Non-MSM spacer, the Mark-BW MSM grid, and the Non-Mixing spacer, respectively.

The ranges of applicability differ slightly from those listed in Reference 1. This is because of the difference in analysis codes (LYNXT used in Reference 1 and XCOBRA-IIIC used here). In Reference 2, the ranges of applicability for the Mark-BW MSM grid were approved as those of the Mark-BW Non-MSM spacer. That practice is followed here but with the XCOBRA-IIIC ranges.

A set of different DNBR design limit values were imposed for different pressure ranges in the approved topical report for the BWU correlation in LYNXT (Reference 1). This conservative practice is followed here by application of the increase in the design limit for each spacer (relative to the design limit in Reference 1) found in the high pressure region (Section 4.1 above) equally in each pressure region. Thus the Mark-BW design limits increase to 1.22 (from

1.19) for pressures above 1000 psia, to 1.23 (from 1.20) for pressures between 700 and 1000 and similarly for the remaining DNBR design limit values.

Table 4.1 BWU-Z Ranges of Applicability
Mark-BW Non-MSM Database

Pressure, psia	400 - 2465
Mass Velocity, Mlb/hr-ft^2	0.352 - 3.577
Thermodynamic Quality at CHF	less than 0.731
Thermal-Hydraulic Computer Code	XCOBRA-IIIC
Spacer	Mark-BW Non-MSM
Design Limit DNBR	
Above 1000 psia	1.22
700 - 1000 psia	1.23
Below 700 psia	1.62
BWU Coefficients	BWU-Z (Table 3.1)

Table 4.2 BWU-Z Ranges of Applicability Mark-BW MSM Database

Pressure, psia	same as Non-MSM Mark-BW
Mass Velocity, Mlb/hr-ft^2	same as Non-MSM Mark-BW
Thermodynamic Quality at CHF	same as Non-MSM Mark-BW
Thermal-Hydraulic Computer Code	XCOBRA-IIIC
Spacer	Mark-BW MSM
Design Limit DNBR	
Above 1000 psia	same as Non-MSM Mark-BW (1.22)
700 - 1000 psia	same as Non-MSM Mark-BW (1.23)
Below 700 psia	same as Non-MSM Mark-BW (1.62)
BWU Coefficients	same as Non-MSM Mark-BW

Table 4.3 BWU-N Ranges of Applicability Non-Mixing Vane Database

Pressure, psia	788 - 2616
Mass Velocity, Mlb/hr-ft^2	0.272 - 3.775
Thermodynamic Quality at CHF	less than 0.690
Thermal-Hydraulic Computer Code	XCOBRA-IIIC
Spacer	Non-Mixing Vane
Design Limit DNBR	
Above 1500 psia	1.22
1200 - 1500 psia	1.31
Below 1200 psia	1.41
BWU Coefficients	BWU-N (Table 3.1)

5.0 References

1. BAW-10199P-A, *The BWU Critical Heat Flux Correlations*, Framatome Cogema Fuels, August 1996.

2. BAW-10199P-A, Addendum 2, *The BWU Critical Heat Flux Correlations*, Framatome Cogema Fuels, August 2000.

3. XN-NF-75-21(P)(A), Revision 2, *XCOBRA-IIIC: A Computer Code to Determine the Distribution of Coolant During Steady-State and Transient Core Operation*, Exxon Nuclear Company, January 1986.

4. BAW-10156-A, Revision 1, *LYNXT Core Transient Thermal-Hydraulic Program*, Babcock & Wilcox, August 1993.

5. ASME Steam Tables, 6th Ed. American Society of Mechanical Engineers, 1993.

6. BAW-10189P, *CHF Testing and Analysis of the Mark-BW Fuel Assembly Design*, Babcock & Wilcox, August 1993.

7. BAW-10143P-A, *BWC Correlation of Critical Heat Flux*, Babcock & Wilcox, April 1985.

8. D. A. Farnsworth and C. D. Morgan, “A Universal CHF Correlation Babcock & Wilcox Fuel,” HDT-Vol. 195, Best Estimate Safety Analysis, National Heat Transfer Conference, ASME, 1992.

9. BAW-10159P-A, *BWCMV Correlation of Critical Heat Flux in Mixing Vane Grid Fuel Assemblies*, Babcock & Wilcox, July 1990.

10. D. A. Farnsworth, “Linearization and Sequential Optimization of Nonlinear Empirical Equations,” Proceedings of the International Topical Meeting on Advances in Mathematics, Computations, and Reactor Physics (Vol. 2), May 1991.

11. Bernard Ostle, *Statistics in Research*, The Iowa State University Press, 1963.

12. M. G. Natrella, *Experimental Statistics*, National Bureau of Standards Handbook, 1963.

13. D. B. Owen, *Factors for One-Sided Tolerance Limits*, Sandia Corporation Monograph, 1963.

Appendix A Detailed Mark-BW Non-MSM Database

Appendix B Detailed Mark-BW MSM Database

Appendix C Detailed BWU-N Non-Mixing Vane Database